

A biophysical basis for inner ear decompression sickness

DAVID J. DOOLETTE¹

SIMON J. MITCHELL²

1. Anaesthesia & Intensive Care, The University of Adelaide,
Adelaide, Australia 5005
2. Department of Anaesthesia, Prince of Wales Hospital,
Sydney, Australia 2031

Address for correspondence: David Doolette
Anaesthesia & Intensive Care
The University of Adelaide
Adelaide Australia 5005
Tel: +61-8-83036382
Fax: +61-8-83033909
Email: David.Doolette@adelaide.edu.au

Running head: Inner ear decompression sickness

Keywords: decompression sickness
labyrinth
nitrogen pharmacokinetics
helium pharmacokinetics
diving

ABSTRACT

Isolated inner ear decompression sickness (DCS) is recognised in deep diving involving breathing of helium-oxygen mixtures, particularly where breathing gas is switched to a nitrogen-rich mixture during decompression. The biophysical basis for this selective vulnerability of the inner ear to DCS has not been established. A compartmental model of inert gas kinetics in the human inner ear was constructed from anatomical and physiological parameters described in the literature and used to simulate inert gas tensions in the inner ear during deep dives and breathing gas substitutions that have been reported to cause inner ear DCS. The model predicts considerable supersaturation, and therefore possible bubble formation, during the initial phase of a conventional decompression. Counterdiffusion of helium and nitrogen from the perilymph may produce supersaturation in the membranous labyrinth and endolymph after switching to a nitrogen-rich breathing mixture even without decompression. Conventional decompression algorithms may result in inadequate decompression for the inner ear for deep dives. Breathing gas switches should be scheduled deep or shallow to avoid the period of maximum supersaturation resulting from decompression.

Keywords: decompression sickness
labyrinth
nitrogen pharmacokinetics
helium pharmacokinetics
diving

INTRODUCTION

Injury to the vestibulo-cochlear apparatus (“inner ear”) during compressed gas diving may be caused by barotrauma, acoustic trauma, or by decompression sickness (DCS). Retrospective reviews of DCS cases in both military (9) and recreational divers (16) suggest that 26% of patients suffering “serious” or “neurological” DCS exhibit evidence of vestibulo-cochlear involvement. These presentations are significant since residual deficits in balance and in hearing are common despite recompression treatment, and the window of opportunity for optimal treatment appears relatively short (3).

The putative cause of inner ear decompression sickness (IEDCS) is bubble formation initiated when the tension (concentration/solubility) of dissolved gas exceeds ambient pressure within the inner ear during ascent. However, beyond this presumed involvement of bubbles there is uncertainty regarding their precise location and effects, or the circumstances under which they are likely to form. Early descriptions of IEDCS following shallow dives often treated ear problems as being of secondary importance to the other central nervous system manifestations of DCS that were almost invariably present. However, the development of deeper diving techniques involving breathing of helium-oxygen gas mixtures has been associated with the occurrence of “pure” or “isolated” IEDCS (7), especially where switches to air or other nitrogen-rich breathing gas mixtures are made to accelerate decompression (3). Indeed, isobaric switches of inspired gas, made while the diver is held at a constant ambient pressure, have precipitated symptoms of IEDCS in the absence of any decompression (10).

This selective vulnerability of the inner ear to DCS under these conditions has been attributed to substantial transfer of highly diffusible helium into the inner ear from the middle ear gas space by diffusion across the round window membrane (7,10). Gas uptake from the middle ear, in addition to that absorbed from the blood, may predispose the inner ear to bubble formation during decompression. Bubble formation might be enhanced or even initiated by

elevated inner ear gas tension resulting from “counterdiffusion” of different gas species of different diffusivity from the blood and middle ear.

We are not aware of any attempts to more formally define the biophysical mechanisms of IEDCS, yet this is an issue of increasing contemporary relevance. Whereas many of the occupational diving tasks that necessitated deep mixed gas diving have now been devolved to remote operated vehicles, there is a new cohort of so-called “technical” recreational divers who are indulging in deep mixed gas “bounce” (short duration, non-saturation) dives in growing numbers. Not surprisingly, reports of isolated IEDCS are starting to emerge from this group.

We present here an illustrative case of isolated IEDCS occurring in a recreational technical diver undertaking a mixed gas dive. We then present a physiological model describing gas kinetics in the inner ear that demonstrates a basis for selective vulnerability of the inner ear to DCS in mixed gas diving. Finally, on the basis of this model, we outline some precautions that may be taken in deep mixed gas bounce diving in order to avoid precipitating IEDCS.

CASE REPORT

A 33 year old male recreational technical diver who had previously made more than 1000 uneventful dives undertook a wreck dive to 110 msw (1201 kPa), 11.9 atmospheres absolute (atm abs), for 25 minutes using a Buddy Inspiration® closed circuit rebreathing SCUBA (A.P. Valves, Helston, Cornwall, U.K.). The diluent gas for the descent, bottom time and the first part of the ascent was trimix comprising 8% oxygen / 60% helium / 32% nitrogen. The diluent was changed to air at 30 msw during the ascent, and the breathing loop was flushed with 100% oxygen at the 4.5 msw stop. The PO₂ set point was 1.3 atm throughout the dive except at the 4.5 msw stop. The dive plan is shown in figure 1, and the diver did not deviate from this plan. The decompression was controlled using a VR3® diver carried computer (Delta P Technology, Poole, Dorset, U.K.) in closed circuit mixed gas mode. These devices operate on the Proplanner® decompression algorithm software (Delta P Technology, Poole, Dorset, U.K.).

The descent, bottom time and the first part of the ascent were uncomplicated. In particular, there were no problems with middle ear equalization. There were no ascent rate violations and no decompression stops were omitted. Shortly after arrival at the 9 msw stop the diver began to experience rotational vertigo. This occurred in short bursts at first, but soon progressed to become persistent. The PO₂ in the rebreather loop at the time was 1.3 atm according to all 3 oxygen sensors. Breathing 50% oxygen / 50% nitrogen using an open circuit SCUBA did not alleviate the problem, and the decompression was continued on the rebreather. The diver became profoundly nauseated and could not keep his eyes open because of the vertigo. He had to alternate between open circuit SCUBA and the rebreather in order to vomit. Despite these debilitating symptoms, he was able to complete the planned decompression stops.

The diver was retrieved onto the boat, given 100% oxygen by demand valve regulator, and evacuated to the nearest recompression chamber where he arrived approximately 4 hours after the onset of symptoms. At this time his vertigo had settled substantially but he remained nauseated. It was still possible to elicit nystagmus on positional testing and he was incapable of performing the Sharpened Romberg Test. An air conduction audiogram revealed normal and symmetrical hearing. There were no other symptoms or signs of DCS or middle ear barotrauma. This appeared to be a case of isolated inner ear (vestibular) DCS.

The diver was recompressed to 4 atm abs and treated according to the protocol specified by the Royal New Zealand Navy Table 1A, which is a modification of the US Navy Air Treatment Table 1A (22) whereby the patient breathes 50% oxygen / 50% helium until decompressed to 2.8 atm abs and breathes 100% oxygen thereafter. This elicited a substantial improvement, but there was persistent mild dysequilibrium for several days after. The diver received 3 once daily follow up treatments consisting of 100% oxygen breathing for 60 minutes at 2.8 atm abs and throughout a 30 minute decompression to 1 atm abs. He has recovered completely (including normalization of his Sharpened Romberg Test) and has made an uneventful return to diving.

METHODS

Physiological model of inner ear inert gas kinetics. A physiological compartmental model of inert gas kinetics in the human inner ear (figure 2) was constructed from parameters in the literature (table 1). Three well-stirred compartments represented the membranous labyrinth, the perilymph, and the endolymph. Inner ear uptake and wash-out of inert gas occurred via perfusion of the membranous labyrinth (vascular compartment) which, unlike the endosteum, is densely vascular (14). Additionally, inert gases diffused between the middle ear gas space and perilymph across the round window membrane, whereas the oval window membrane was considered occluded by the ossicles. Within the inner ear, inert gas diffused between the vascular compartment and each labyrinthine fluid compartment. Diffusion-limiting membranes of zero volume notionally separated the compartments and the middle ear; the flows of inert gases across these membranes (table 2) were formulated to reflect a slab approximation to the diffusion geometry (A/h , table 1) of the labyrinthine fluid compartments. Diffusivities and solubilities of nitrogen and helium in blood, tissue, and labyrinthine fluids were characteristic of aqueous tissues. This compartmental approximation of diffusion does not consider transient inert gas tension gradients within the tissues represented by the compartments but provides an effective first order approximation to the volume averaged inert gas tensions (20). Model input comprised arterial inert gas tensions and middle ear inert gas partial pressures, both being considered to equilibrate instantly with inspired inert gas partial pressures adjusted for water vapour pressure at 37°C.

Not all parameter values for the human inner ear model were available in the literature and some were estimated or scaled from animal data. Blood flow was scaled up from measurements made on guinea pig inner ear (17) which is one tenth the volume of the human inner ear (8,21). Vascular compartment volume was derived from blood flow using values of tissue perfusion ($\text{mL} \times 100 \text{ g}^{-1} \times \text{min}^{-1}$) for rat cochlea and vestibular sensory organs (13).

Doubling or halving these two parameters resulted in only small quantitative but not qualitative differences in model simulations. The diffusion geometry (A/h, table 1) of the labyrinthine fluid compartments was based on modelling the endolymph and perilymph volumes as being contained in concentric tubes of 0.025 cm (h_{end}) and 0.058 cm ($h_{per}+h_{end}$) radius respectively, separated by the membranous labyrinth tissue which has a surface area of A_{vas} on each face. The diffusion distance from the round window (h_{rw}) was based on the radius of a sphere of inner ear volume ($V_{end}+V_{per}+V_{vas}$).

The model was written as the following ordinary differential equations for each inert gas:

$$S \times V_{vas} \times \frac{dP_{vas}}{dt} = Q \times S \times (P_a - P_{vas}) - PSA_{per} \times (P_{vas} - P_{per}) - PSA_{end} \times (P_{vas} - P_{end})$$

$$S \times V_{per} \times \frac{dP_{per}}{dt} = PSA_{per} \times (P_{vas} - P_{per}) - PSA_{rw} \times (P_{per} - P_{me})$$

$$S \times V_{end} \times \frac{dP_{end}}{dt} = PSA_{end} \times (P_{vas} - P_{end})$$

Where P_{vas} , P_{per} , P_{end} , and P_a are the vascular, perilymph, endolymph, and arterial blood inert gas tensions, P_{me} is the middle ear inert gas partial pressure, $PSA = D \times S \times A/h$ are the relevant flow values given in table 2, and all other abbreviations are defined in table 1. Simulations were performed using Scientist for Windows [computer program] (version 2.01. Salt Lake City (UT): Micromath Inc.; 1995).

Validation of the model. There are no measurements of inner ear inert gas kinetics to validate the model against; however, oxygen, which has similar diffusivity to nitrogen, has been measured in the labyrinthine fluids using polarographic electrodes. One such report gives the initial slope of the decline of oxygen tension in the guinea pig cochlea perilymph and endolymph during anoxia (19). Assuming zero vascular compartment oxygen tension, these data can be used to calculate approximate time constants = initial tension/(-initial slope) for

diffusion of oxygen from the guinea pig endolymph of 30 s and from the perilymph of 44 s; these are of the same order as the derived nitrogen time constants in the present human model.

RESULTS

Simulations using the inner ear model. Figure 3 shows a simulation of the gas tensions in the inner ear model compartments during an isobaric gas switch reported to result in DCS (10). After a full day residence at 37.4 atm abs breathing the chamber atmosphere of 0.21 atm oxygen, balance helium, with no change in ambient pressure, the subject began breathing 0.21 atm oxygen, 10 atm nitrogen, balance helium through a mask, during which severe nausea, vomiting and vertigo developed. The breathing gas switch results in a transient elevation of vascular compartment and endolymph gas tensions above ambient pressure; such supersaturation is required for bubble formation. The peak vascular compartment gas tension was 37.8 atm (0.4 atm supersaturation) occurring at 2 minutes after the gas switch.

In figure 3 and other simulations of isobaric breathing gas switches after blood:tissue equilibrium, the peak change in inner ear vascular compartment gas tension from equilibrium was approximately 4.8% of the change in arterial nitrogen tension, expressed in terms of inspired gas for a switch from breathing gas 1 to 2 as $0.048 \times (P_{IN_2-2} - P_{IN_2-1}) \times (1 - P_{H_2O}/P_{amb})$, where P_{amb} is ambient pressure and P_{H_2O} is saturated water vapor pressure at 37°C. At equilibrium the total tissue gas tension equals dry inspired inert gas partial pressure $(P_{amb} - P_{IO_2}) \times (1 - P_{H_2O}/P_{amb})$ plus the tissue metabolic gas tensions $(P_{tisO_2} + P_{tisCO_2} + P_{H_2O})$. For an isobaric switch peak supersaturation (total tissue gas tension - P_{amb}) is: $(0.048 \times (P_{IN_2-2} - P_{IN_2-1}) - P_{IO_2}) \times (1 - P_{H_2O}/P_{amb}) + P_{tisO_2} + P_{tisCO_2}$. The peak supersaturation depends on the magnitude of the inert gas substitution and the inspired oxygen tension since tissue oxygen tension is relatively independent of inspired oxygen partial pressures used in diving.

The transient increase in gas tension following a substitution of nitrogen for helium in breathing gas results from the difference in gas transfer between compartments (table 2). The flow of nitrogen into the vascular compartment via the arterial blood exceeds washout of

helium in venous effluent. The transfer of helium into the vascular compartment by diffusion from the perilymph and endolymph exceeds the counterdiffusion of nitrogen in the opposite direction and temporarily exceeds the washout of helium in the blood.

Examination of the flows and time constants in table 2 indicates that transfer of nitrogen and helium across the round window is negligible in comparison to the other transport processes. The time constant is related to the flow by $V \times S / \text{flow}$ and by definition 99% equilibration by this process alone occurs in 4.6 time constants. Whereas the round window is only 70 μm thick (5) and likely freely permeable to inert gases, owing to the large diffusion distances through the inner ear fluid spaces, transfer of gas via this route had little effect on the inner ear compartment gas tensions over the time course of the present simulations. The time constants for transfer of inert gases between the vascular compartment and the labyrinthine fluids are sufficiently large that considerable inert gas tension gradients across endolymph and perilymph may persist over the time course of the present simulations.

Although a multi-compartmental model, the gas kinetics of the entire inner ear for longer time periods can be approximated from the overall perfusion time constant, equivalent to a half time of 8.8 min ($\ln 2 \times \text{TC}$). Similar kinetics are illustrated in figure 1 which shows, in addition to the depth/time profile of the dive reported in the case history, the inner ear gas tensions simulated according to the present model. This simulation indicates considerable supersaturation during the early (deep) phase of decompression. For clarity at this scale, only the vascular compartment is illustrated. This half time is quite slow in comparison to a well-perfused tissue such as brain, which would have a half time of 1.7 min (assuming brain blood perfusion of $40 \text{ mL} \times 100 \text{ g}^{-1} \times \text{min}^{-1}$). The magnitude of counterdiffusion effect during the switch from trimix to air diluent at 4 atm abs (51 minutes in figure 1) is modest because the partial pressure of nitrogen substituted for helium is small, and is manifest only as a transient

slowing of gas washout, not evident at this scale in figure 1. However the breathing gas switch from trimix to air diluent occurred while the inner ear vascular compartment was already supersaturated (1.09 atm) due to decompression and shortly following the time of maximum supersaturation (1.7 atm) at 44 minutes and 4.6 atm abs.

DISCUSSION

The case described here typifies the type of technical recreational diving that is becoming increasingly widespread. It also illustrates the potential for isolated IEDCS to occur in a seemingly random fashion during an otherwise uneventful deep technical dive that has gone according to plan. As we will discuss below, this case and others like it suggest that some decompression algorithms for deep technical dives, particularly those incorporating switches to nitrogen-rich breathing gas, may need to be modified in order to avoid such events. It certainly seems possible that isolated IEDCS will become more common as technical diving grows in popularity.

IEDCS is a poorly defined clinical entity and is difficult to study epidemiologically. One of the principal difficulties is that several distinct pathological processes may produce the same symptoms and there is no gold standard test for distinguishing between them. In particular, there is frequent difficulty distinguishing between isolated IEDCS and inner ear barotrauma (barotraumas are tissue damage caused by compression or expansion of adjacent gas spaces). Clinicians must rely on interpretations of the circumstances of the dive as well as on the features of the illness itself in order to come to a diagnosis, but ambiguity is common. It is an important distinction since the DCS patient requires recompression whereas recompression is relatively contraindicated in inner ear barotrauma (16). Distinguishing the source of vestibulo-cochlear symptoms in DCS patients with obvious widespread neurological involvement is also difficult, since it is possible that central rather than end-organ lesions may be involved. Clinically this distinction is less important since all DCS patients require recompression, but such cases complicate epidemiological analyses of IEDCS.

Notwithstanding these difficulties, both the case presented here and those in the series published by Farmer et al (1976) provide reasonable evidence that end organ IEDCS exists as an isolated pathological entity. None of these cases experienced any difficulty with middle

ear equalization or exhibited any evidence of middle ear barotrauma; nor were there any other neurological symptoms suggestive of a central nervous system involvement. Moreover, since those discrete cerebral and cerebellar areas responsible for vestibulo-cochlear function exhibit no unique characteristics that would influence gas kinetics, it seems unlikely that symptomatic bubble formation would manifest only in those areas. Isolated inner ear damage is a more plausible explanation for these cases. Inner ear damage has been demonstrated by *in vivo* studies in guinea pigs (15) and squirrel monkeys (11) subjected to decompression.

Although isolated IEDCS has been described following relatively shallow air diving (16) it appears to be more commonly associated with deep helium-oxygen diving (2,4). IEDCS onset has been described either early during the initial rapid phase of decompression from very deep dives (150 to 300 msw) while still breathing helium-oxygen, or following a switch to air breathing at shallower depths (2,4).

IEDCS may be associated with deep diving because a considerable gas burden must be acquired to cause symptoms. The model proposed here suggests an inner ear half time (8.8 min) that allows considerable gas uptake during a deep dive and considerable supersaturation, and potentially bubble formation, in all inner ear compartments during the initial rapid phases of decompression. Many decompression algorithms, including the ZH-L16 (1) that forms the basis of many technical diving decompression algorithms including the Proplanner® used in the present case report, control decompression according to the rule $P_{tis} < W \times P_{amb} + Z$ where P_{tis} is the total inert gas tension in a compartment and W and Z are constants. Although such rules can be empirically derived without biophysical assumptions, they have also been interpreted as describing a critical volume of released gas (bubbles) causing DCS (6). In this case, by mass balance of the amount of inert gas in the compartment immediately prior to and following just critical bubble formation, $W = 1 + V_c/S$ and $Z = W \times (P_e + P_{st} - P_{tisO_2} - P_{tisCO_2} - P_{H_2O})$,

where V_c is the critical volume of gas, S is the solubility of inert gas in the tissue, P_e and P_{st} are pressures opposing bubble formation due to tissue deformation and surface tension, respectively. Isolated IEDCS would selectively occur following deep dives and earlier than expected during decompression if the constant W were small and Z were large in comparison to the compartments responsible for other symptoms of DCS (6). It seems plausible that V_c (and therefore W) might be small in the inner ear, which, as a sensitive transducer of mechanical energy, may be disrupted by small volumes of bubbles. Furthermore, P_e (and therefore Z) may be large since the inner ear is composed primarily of incompressible liquid within a non-distensible bony capsule with only small canal outlets.

The association of IEDCS with helium-oxygen diving in the absence of breathing gas switches may be coincidental since helium-oxygen breathing is standard practice for deep diving. However, IEDCS is clearly associated with switching breathing gas from helium to nitrogen rich mixtures (4,10), and the present model suggests such gas substitution may cause bubble formation in the membranous labyrinth and endolymph. The model implicates transient supersaturation resulting from a counterdiffusion mechanism in which helium transfer from the perilymph to the other compartments temporarily exceeds the washout of helium in the venous blood. This transient mechanism is analogous to the steady-state “counter perfusion” mechanism proposed by Hills (1977). The anatomical requirements for this phenomenon are a large, diffusion-limited source of helium adjacent to a tissue with a relatively small blood supply and are provided by the perilymph surrounded by the smaller volume of vascular membranous labyrinth. Conversely, theoretical treatment of a more typical tissue arrangement such as muscle capillary unit suggest a transient under-saturation of tissue could result from switching breathing gas from helium to nitrogen rich mixtures (23). It is on similar premise that such breathing gas switches are used to accelerate decompression.

The present model suggests diffusion of middle ear gas across the round window is negligible although previously proposed mechanisms implicated steady state counterdiffusion of atmospheric helium and blood nitrogen across the round window and tympanic membranes (7,10). This previous proposal appears to have been made by analogy with the production of dermal lesions and continuous production of venous gas emboli by steady state counterdiffusion across the skin in humans or animals exposed to a helium atmosphere while breathing a different inert gas without decompression (10).

The present model of dissolved inert gas kinetics is not a complete model of inner ear decompression; for instance it does not explain the 50-minute delay between predicted maximum supersaturation and onset of symptoms of IEDCS in the present case report. This delay may be related to the dynamics of bubble growth due to gas influx and expansion during decompression or biological processes induced by bubbles that are not considered in the present model. Nevertheless, the present physiological model can be used to deduce some qualitative implications for scheduling of technical deep diving decompression. First, the use of some decompression algorithms to plan very deep bounce dives (arbitrarily in excess of 100 msw) may result in inadequate decompression for the inner ear and may require, for instance, adjustment of W and Z constants for compartments with half times near 8.8 minutes as described. This would typically result in deeper decompression stops. Second, breathing gas switches from helium-rich to nitrogen-rich mixtures will produce an over-saturation in the inner ear that increases with depth and decreasing inspired oxygen partial pressure. Such breathing gas switches should be carefully scheduled either deep (with due consideration to nitrogen narcosis) or shallow to avoid the period of maximum supersaturation resulting from the decompression (Figure 1). Switches should also be made whilst breathing the largest inspired oxygen partial pressure that can be safely tolerated with due consideration to oxygen toxicity.

ACKNOWLEDGMENTS

This work was supported in part by a Jean B Reid Research Associateship, Health Science Research Committee, the University of Adelaide.

REFERENCES

1. **Bühlmann AA.** Die Berechnung der risikoarmen Dekompression. *Schweiz Med Wschr* 118: 185-197, 1988.
2. **Bühlmann, A. A. and Gehring, H.** Inner ear disorders resulting from inadequate decompression - "vertigo bends". In: *Underwater Physiology V*, edited by Lambertsen CJ. Bethesda: FASEB, 1976.
3. **Farmer JC, Thomas WG, Youngblood DG, and Bennett PB.** Inner ear decompression sickness. *Laryngoscope* 86: 1315-1327, 1976.
4. **Farmer JC, Jr.** Diving injuries to the inner ear. *Ann Otol Rhinol Laryngol Suppl* 86: 1-20, 1977.
5. **Goycoolea MV.** Clinical aspects of round window membrane permeability under normal and pathological conditions. *Acta Otolaryngol* 121: 437-447, 2001.
6. **Hennessy TR and Hempleman HV.** An examination of the critical released gas volume concept of decompression sickness. *Proc R Soc Lond B Biol Sci* 197: 229-313, 1977.
7. **Hills BA.** *Decompression Sickness: The biophysical basis of prevention and treatment.* Chichester: John Wiley & Sons, 1977.
8. **Igarashi M, Ohashi K, and Ishii M.** Morphometric comparison of endolymphatic and perilymphatic spaces in human temporal bones. *Acta Otolaryngol* 101: 161-164, 1986.
9. **Kennedy RS and Diachenko JA.** Incidence of vestibular symptomatology in 2,500 U.S. Navy diving accidents (1933-1970). *Aviat Space Environ Med* 46: 432-435, 1975.
10. **Lambertsen CJ and Idicula J.** A new gas lesion syndrome in man, induced by "isobaric gas counterdiffusion". *J Appl Physiol* 39: 434-443, 1975.
11. **Landolt JP, Money KE, Topliff ED, Nicholas AD, Laufer J, and Johnson WH.** Pathophysiology of inner ear dysfunction in the squirrel monkey in rapid decompression. *J Appl Physiol* 49: 1070-1082, 1980.

12. **Lango T, Morland T, and Brubakk AO.** Diffusion coefficients and solubility coefficients for gases in biological fluids: a review. *Undersea Hyperb Med* 23: 247-272, 1996.
13. **Lyon MJ and Jensen RC.** Quantitative analysis of rat inner ear blood flow using the iodo[(14)C]antipyrine technique. *Hear Res* 153: 164-173, 2001.
14. **Mazzoni A.** The vascular anatomy of the vestibular labyrinth in man. *Acta Otolaryngol Suppl* 472: 1-83, 1990.
15. **McCormick JG, Philbrick T, Holland W, and Harrill JA.** Diving induced sensori-neural deafness: Prophylactic use of heparin and preliminary histopathology results. *Laryngoscope* 43: 1483-1501, 1973.
16. **Nachum Z, Shupak A, Spitzer O, Sharoni Z, Doweck I, and Gordon CR.** Inner ear decompression sickness in sport compressed-air diving. *Laryngoscope* 111: 851-856, 2001.
17. **Nakashima T, Suzuki T, Morisaki H, and Yanagita N.** Blood flow in the cochlea, vestibular apparatus and facial nerve. *Acta Otolaryngol* 111: 738-742, 1991.
18. **Okuno H and Sando I.** Anatomy of the round window. A histopathological study with a graphic reconstruction method. *Acta Otolaryngol* 106: 55-63, 1988.
19. **Prazma J.** Perilymphatic and endolymphatic PO₂. Variations during anoxia, hyperoxia, and hypercapnia. *Arch Otolaryngol* 108: 539-543, 1982.
20. **Scheid P, Meyer M, and Piiper J.** Elements for modeling inert gas washout from heterogeneous tissues. *Adv Exp Med Biol* 180: 65-72, 1984.
21. **Shinomori Y, Spack DS, Jones DD, and Kimura RS.** Volumetric and dimensional analysis of the guinea pig inner ear. *Ann Otol Rhinol Laryngol* 110: 91-98, 2001.
22. *U.S. Navy Diving Manual (Air Diving).* Revision 1. Washington DC: Naval Sea Systems Command, 1985.
23. **Young C and D'Aoust BG.** Factors determining temporal pattern of isobaric supersaturation. *J Appl Physiol* 51: 852-857, 1981.

LEGENDS

Figure 1. Pressure-time schedule for the case report mixed gas rebreather technical dive (ambient pressure in atm abs, solid line) that resulted in isolated IEDCS. The predicted inner ear vascular compartment (membranous labyrinth) dissolved gas tension (atm) is shown as the dashed line. Dissolved gas tension includes model predictions of nitrogen and helium tensions plus a fixed value (0.19 atm) representing metabolic gas tensions ($P_{tisO_2} + P_{tisCO_2} + P_{H_2O}$).

Figure 2. Physiological compartmental model of inner ear dissolved inert gas kinetics. Boxes with propellers indicated the well-stirred endolymph, vascular (membranous labyrinth), and perilymph compartments. Single headed arrows indicate the direction of flows of inert gases by perfusion with blood. Double headed arrows indicate the directions of flows of inert gas by diffusion. P_a (arterial blood inert gas tensions) and P_{me} (middle ear inert gas tensions) represent the model inputs.

Figure 3. Model simulation of an isobaric breathing gas switch from helium-oxygen to helium-nitrogen-oxygen that resulted IEDCS as described in results. Dissolved gas tensions (atm) in the three model compartments are shown as solid lines. The horizontal dashed line indicates the ambient pressure (atm abs).

TABLE 1. MODEL PARAMETERS

Parameter	Description	Value	Reference
V_{end}	Endolymph compartment volume	0.0388 mL	(8)
V_{per}	Perilymph compartment volume	0.166 mL	(8)
V_{vas}	Vascular compartment volume	0.070 mL	*
Q	Inner ear blood flow	$0.00036 \text{ mL} \times \text{s}^{-1}$	*
A_{vas}	Vascular compartment surface area	3 cm^2	*
A_{rw}	Round window surface area	0.022 cm^2	(18)
h_{end}	Diffusion distance	0.025 cm	*
h_{per}	Diffusion distance	0.033 cm	*
h_{rw}	Diffusion distance	0.4 cm	*
S_{He}	Helium solubility	$0.01 \text{ mL} \times \text{mL}^{-1} \times \text{atm}^{-1}$	(12)
S_{N_2}	Nitrogen solubility	$0.015 \text{ mL} \times \text{mL}^{-1} \times \text{atm}^{-1}$	(12)
D_{He}	Helium diffusivity	$3.94 \times 10^{-5} \text{ cm}^2 \times \text{s}^{-1}$	(12)
D_{N_2}	Nitrogen diffusivity	$1.3 \times 10^{-5} \text{ cm}^2 \times \text{s}^{-1}$	(12)

*Derived values, see text.

TABLE 2. COMPARTMENT TIME CONSTANTS AND FLOWS

	Time constant		Flow	
	Formula	Value s	Formula	Value mL \times s $^{-1}$ \times atm $^{-1}$
Vascular- endolymph	$h_{\text{end}}^2/D_{\text{N}_2}$	48	$D_{\text{N}_2}\times S_{\text{N}_2}\times A_{\text{vas}}/h_{\text{end}}$	2.34×10^{-5}
	$h_{\text{end}}^2/D_{\text{He}}$	16	$D_{\text{He}}\times S_{\text{He}}\times A_{\text{vas}}/h_{\text{end}}$	4.73×10^{-5}
Vascular- perilymph	$h_{\text{per}}^2/D_{\text{N}_2}$	84	$D_{\text{N}_2}\times S_{\text{N}_2}\times A_{\text{vas}}/h_{\text{per}}$	1.77×10^{-5}
	$h_{\text{per}}^2/D_{\text{He}}$	28	$D_{\text{He}}\times S_{\text{He}}\times A_{\text{vas}}/h_{\text{per}}$	3.58×10^{-5}
Middle ear- perilymph	$(h_{\text{rw}}\times V_{\text{ie}})/(D_{\text{N}_2}\times A_{\text{rw}})$	3.83×10^5	$D_{\text{N}_2}\times S_{\text{N}_2}\times A_{\text{rw}}/h_{\text{rw}}$	1.07×10^{-8}
	$(h_{\text{rw}}\times V_{\text{ie}})/(D_{\text{He}}\times A_{\text{rw}})$	1.26×10^5	$D_{\text{He}}\times S_{\text{He}}\times A_{\text{rw}}/h_{\text{rw}}$	2.17×10^{-8}
Vascular perfusion	V_{vas}/Q	194	$Q\times S_{\text{N}_2}$	5.40×10^{-6}
			$Q\times S_{\text{He}}$	3.6×10^{-6}
Inner ear perfusion	V_{ie}/Q	761		

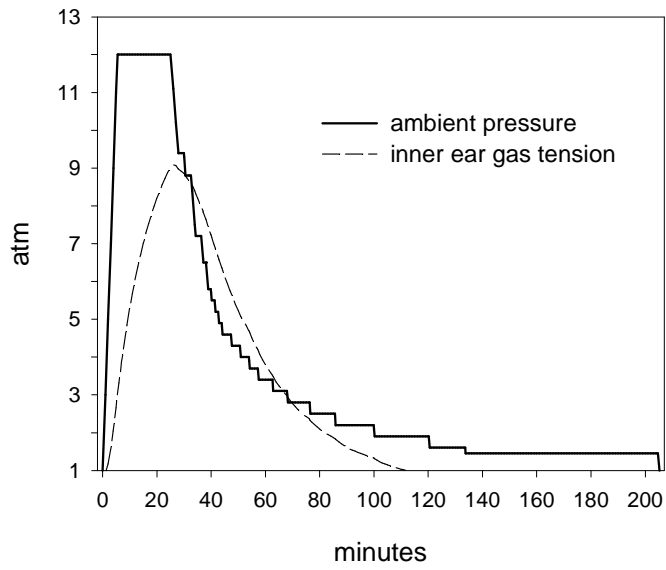


figure 1

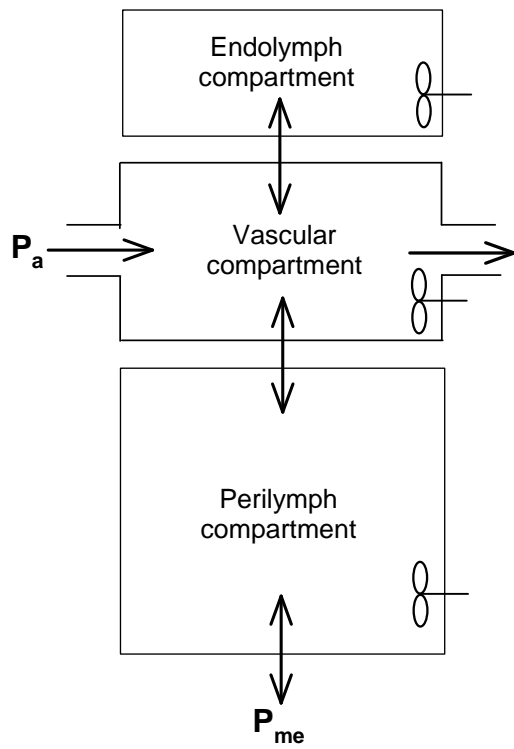


figure 2

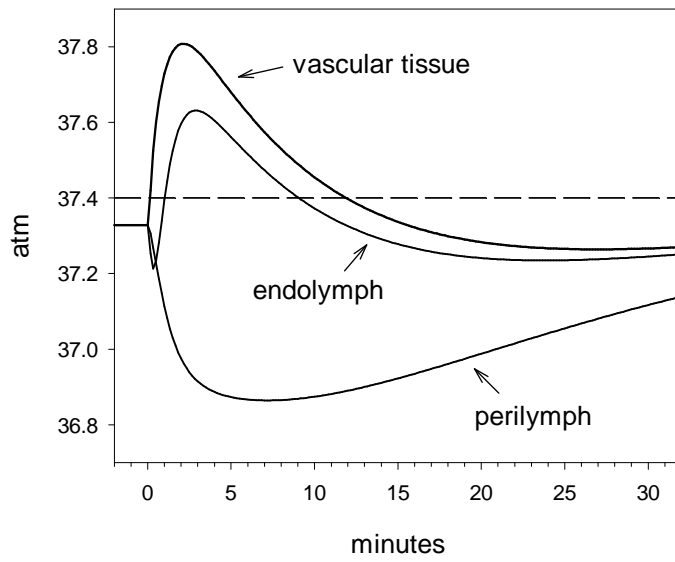


figure 3